ACS Macro Letters

Letter

pubs.acs.org/macroletters

# Enhanced Light Absorption in Porous Particles for Ultra-NIR-Sensitive Biomaterials

Jian Wang,[†] Jing Zhao,[†] Yanbo Li,[‡] Man Yang,[‡] Yu-Qiang Chang,[†] Jian-Ping Zhang,[†] Zhiwei Sun,*[,‡] and Yapei Wang*[,†]

[†]Department of Chemistry, Renmin University of China, Beijing 100872, P. R. China

[‡]School of Public Health and Family Medicine, Capital Medical University, Beijing 100069, P. R. China

Supporting Information

**ABSTRACT:** Conducting polymers with the capability of photothermal conversion extend the application of near-infrared light (NIR), satisfying the demands of less toxicity, easy availability, and high flexibility for NIR-sensitive materials. The improvement of light use efficiency is still urgent and challenging. In this work, an ultra-NIR-sensitive biocompatible porous particle composed of a polylactic acid matrix and polypyrrole nanoparticles is prepared via a one-step double-emulsion method. It is revealed that the light absorption of polyprryole is effectively improved within the porous structure. This particle is exploited as a cost-effective sensing material in terms of its conductivity change for preparing paper-based NIR light sensors. Moreover, the microspheres act as a guardian to encapsulate and lock excess nucleic acids which is useful for preventing inflammatory diseases.

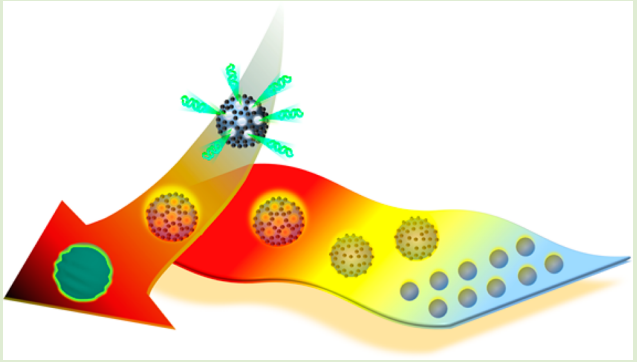

Near-infrared light is of great use in many areas including bioimaging,[1,2] tumor ablation,[3] diagnosis, and military surveillance[4,5] owing to its deep tissue penetration and low atmosphere adsorption.[6,7] Great efforts have been devoted to exploring materials with the absorbance in the near-infrared region.[8,9] In addition to two-photon absorption and up-conversion,[10,11] photothermal conversion is becoming a powerful way to use NIR light in high efficiency. Photothermal conversion is generally built on low-band-gap materials without the evidence of luminescent emission under NIR irradiation.[12−15] Inorganic semiconductors showing high thermodynamic stability and light sensitivity have been extensively used, while problems of limited flexibility and toxicity are encountered.[16] Conducting polymers with dark color were recognized as a particular class of NIR-sensitive materials, meeting the demands of less toxicity, easy availability, and high flexibility. These dark polymers are able to adsorb light and convert photoenergy to thermal heat. Most attention has been paid to their use of thermal heating. We recently demonstrated that photothermal conversion can also induce the change of their conductivity, offering an opportunity for preparing low-cost and flexible light sensors.[17−19] However, NIR-sensitive devices are still at the laboratory level, and the detection sensitivity is not satisfactory. In view of the demand of low light dose in biological systems, the improvement of photothermal conversion efficiency is essential to realize their full potential for clinical use.

Enhancing the light absorption is an effective way to improve the light conversion efficiency. Natural systems are remarkably efficient at this process.[20−23] An example of the polar bear illustrates that microstructures can tailor the reinforcement of light adsorption. This anticold animal has hollow hairs and dark skin. Light can be trapped by the hollow hair with negligible waste, leading to highly efficient photothermal conversion by passing through the skin.[24] With this inspiration, we integrate dark materials of polypyrrole with a porous polymer matrix intending for the preparation of ultra-NIR-sensitive materials. Porous structures have shown the functions of light scattering and diffraction that prolong the path length of light in optoelectronic devices.[25,26] We proposed that the enhancement of light trapping by porous structure will facilitate polypyrrole to absorb more photon energy, hence improving the efficiency of photothermal conversion.

In this work, we demonstrated an easy way to prepare a porous scaffold for supporting NIR-sensitive polypyrrole. As outlined in Figure 1, a one-step emulsion method was developed to build porous polymer particles with surface coated by polypyrrole nanoparticles (PPy NPs). An oil phase consisting of dichloromethane, poly(lactic acid) (PLA), and pyrrole was dispersed in a water phase. Instead of traditional surfactants, a deprotonated natural protein of bovine albumin (BSA) was included in the water phase acting as the emulsifier in terms of its biocompatibility. A W/O/W double emulsion system was quickly formed after a vigorous agitation. This

**Received:** February 5, 2015
**Accepted:** March 20, 2015
**Published:** March 23, 2015





DOI: 10.1021/acsmacrolett.5b00089
*ACS Macro Lett.* 2015, 4, 392−397

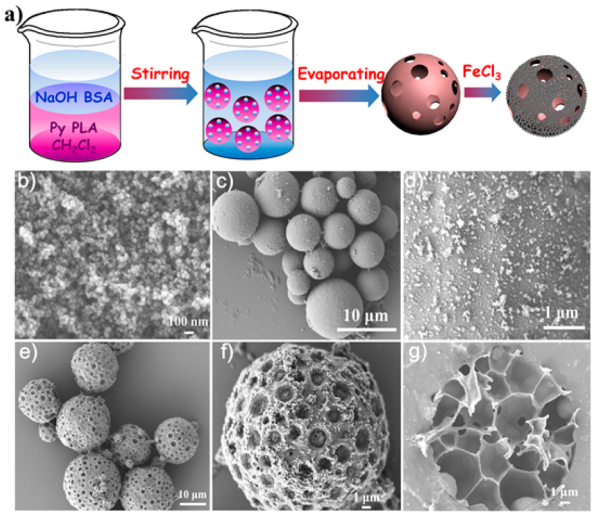


**Figure 1.** (a) Schematic illustration of the double emulsion method for preparing PPy@PLA particles. SEM images of (b) PPy NPs, (c, d) solid PLA particles coated with PPy NPs prepared at pH 7, and (e, f) porous PLA particles coated with PPy NPs prepared at pH 12. The cross-section of the porous PLA particle (g) is visualized by opening particles within an epoxy resin.

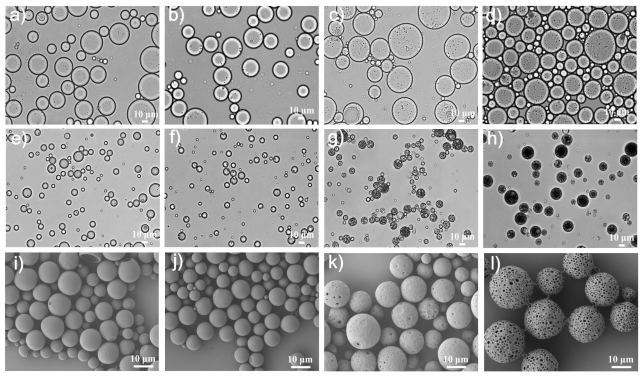


**Figure 2.** Optical microscopic images of emulsions under different pH conditions and their solid products after solvent evaporation: (a, e) pH = 1; (b, f) pH = 7; (c, g) pH = 10; (d, h) pH = 12. The concentration of PLA and BSA is 50 and 5 mg/mL, respectively. Oil–water ratio is 1:3. SEM images of the PLA particle that were prepared by the emulsions at (i) pH = 1, (j) pH = 7, (k) pH = 10, and (l) pH = 12, respectively.

emulsion is thermodynamically stable such that phase separation is not notable in a few days. The volatile dichloromethane was evaporated at 40 °C, solidifying the PLA matrix into porous particles. Yet pyrrole still remained in the polymer matrix which could be polymerized upon addition of $FeCl_3$. As shown in Figure 1e and 1f, a layer of polypyrrole nanoparticles was formed on the surface of PLA porous particles after polymerization for 45 min. However, few PPy NPs were observed in the interior of PLA particles (Figure 1g). It is assumed that the polymerization of pyrrole mainly happens at the interface due to the poor penetration of oxidant into the polymer matrix. As a control, PPy NPs were synthesized by a single emulsion using pyrrole as the oil phase and BSA as the emulsifier.

The pH value in the water phase has a great effect on the morphology of PPy@PLA particles. As shown in Figure 1c and 1d, at a given BSA concentration and oil–water ratio, solid PLA particles coated with PPy NPs yet without open surface pores were formed after the processes of emulsification and polymerization at neutral conditions. In order to understand the pH effect on the particle morphology, the water–oil mixtures with the same compositions were emulsified at different pH conditions. As shown in Figure 2, single O/W emulsions exist at pH below 7, while W/O/W double emulsions were observed at basic conditions. The inner water phase in the double-emulsion systems acts as soft templates, leading to the formation of porous structures after solvent evaporation. On the contrary, nonporous particles were formed after solvent evaporation of single emulsions. It is an abnormal phenomenon that double emulsions could be formed by one-step emulsification with the use of a single surfactant. Considering PLA is terminated by carboxyl acid, we hypothesize that PLA becomes amphiphilic when the terminal carboxyl acid is deprotonated at basic conditions. Hence the interfacial equilibrium is reorganized which induces the phase inversion. This hypothesis is identified by a Pendant drop study of interfacial tension between dichloromethane containing PLA and water without BSA. As shown in Figure S1 (Supporting Information), the interfacial energy indicative of the interfacial activity of PLA drops upon the increase of pH value. PLA can stabilize an emulsion between dichloromethane and water at pH 12 even more (Figure S3, Supporting Information).

To validate that the porous structure can tailor the enhancement of NIR light adsorption by polypyrrole, the light sensitivities of PPy NPs on PLA particles were thoroughly assessed at a range of power densities. Three kinds of particles including PPy NPs, nonporous PPy@PLA, and porous PPy@PLA were deposited onto cellulose paper using a suction filtration method.[27] PPy NPs have a remarkable absorption within the NIR region (Figure 3a), and they are supposed to be electrically active to NIR light owing to the photothermal conversion. The light sensitivity of these paper chips with the active PPy NP layers could be evaluated by bridging them into electrical circuits. To do that, the particle layer was sputtered with two gold electrodes and connected to an electrochemical workstation. The electrical response is followed by the relative change of conductivity ($\Delta G/G_0$ (%)) under NIR illumination as shown in eq 1

$$\Delta G/G_0\ (\%) = [(I - I_0)/I_0] \times 100 \qquad (1)$$

where $I_0$ represents the initial current before the NIR illumination, and $I$ is the current under NIR illumination with a specific power density. The contents of polypyrrole on nonporous PPy@PLA and porous PPy@PLA particles are 36.1 and 34.0 wt %, respectively. As such, the mass of light-active polypyrrole on cellulose paper could be governed, which is retained consistent (0.3 mg/cm$^2$) on each paper chip in order to emphasize the contribution of particle morphology to the light sensing. As shown in Figure 3b, the porous PPy@PLA particles are more sensitive to NIR light than PPy NPs and nonporous PPy@PLA particles. The relative conductivity change reached 40% when the paper sensor consisting of porous PPy@PLA particles was exposed to light with power density of 1 W/cm$^2$, higher than 20% by nonporous PPy@PLA particles and 10% by PPy NPs. It should be noted that porous PPy@PLA particles always produce greater electrical signal than nonporous PPy@PLA particles or PPy NPs at a given light power (Figure 3c), indicating the porous structure has a positive effect on light sensing.



DOI: 10.1021/acsmacrolett.5b00089
*ACS Macro Lett.* 2015, 4, 392–397

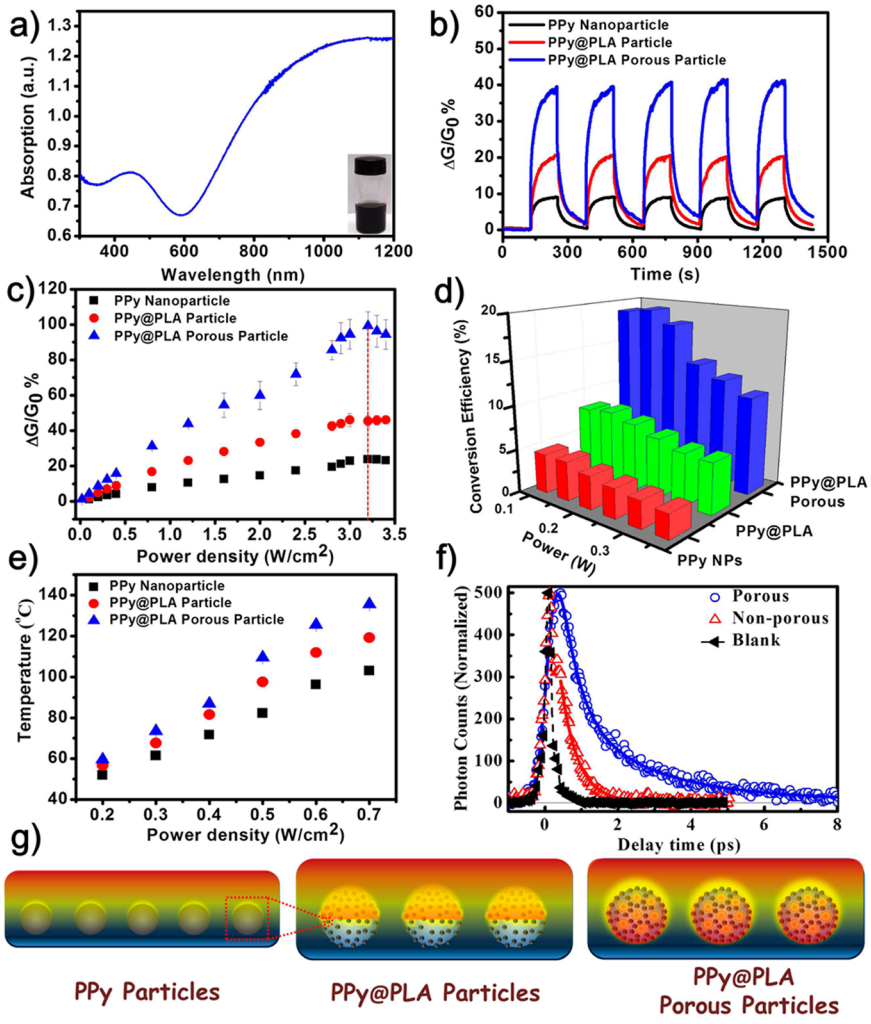


**Figure 3.** (a) UV−vis−NIR absorption of PPy NPs in aqueous solution. The concentration of the nanoparticles is 300 $\mu$g/mL. (b) NIR-light sensing test cycles of paper chips consisting of PPy NPs, PPy@PLA, or porous PPy@PLA particles. Light power density is 0.1 W/cm$^2$. (c) The relative conductivity change under different light power density ranging from 0.01 to 3.5 W/cm$^2$. (d) Photothermal conversion efficiency deduced by the method of differential scanning calorimetry under different temperatures. (e) Surface temperature changes of three different kinds of paper chips under different power densities ranging from 0.2 to 0.7 W/cm$^2$ with light irradiation for 15 s. (f) Temporal evolution profiles of femtosecond laser pulses (120 fs, 800 nm) reflected from the blank substrate and the thin films of porous and nonporous PLA spheres. (g) A schematic illustration of porous morphology enhancing the light adsorption of polypyrrole.

The increase of conductance upon NIR irradiation is attributed to the photothermal conversion of polypyrrole. It is assumed that both number and mobility of effective carriers are increased as a result of the increased temperature by photothermal conversion. As shown in Figure 3d, the local temperature of the active PPy layer quickly increases under light illumination. The contribution of porous structure was quantified by the evaluation of photothermal conversion efficiency ($\eta$) which meets eq 2 as follows

$$\eta = \frac{Q}{E} = \frac{Q}{P \times t} \tag{2}$$

where $Q$ is the Joule heat of the PLA matrix, and $E$ and $P$ refer to the total photoenergy and power of the NIR laser, respectively. The heat energy ($Q$) is defined by the specific heat ($C_p(T)$), temperature ($T$), and mass ($m$) of PLA particles. The specific heats of PLA and PLA with PPy NPs were estimated as a function of heat flow (HF) through the method of differential scanning calorimetry (DSC) (Figure S10, Supporting Information), which is shown as follows

$$C_p = \frac{\mathrm{HF}}{M \cdot \beta} \tag{3}$$

$$Q = m \int_{T_0}^{T} C_p(T)\mathrm{d}T \tag{4}$$

where $\beta$ refers to the heating rate, and $M$ refers to the mass of the samples being tested in the DSC experiment. Joule heat ($Q$) could be obtained by integrating the DSC curves from a given temperature interval. As shown in Figure 3d, porous PLA@PPy NPs exhibit higher photothermal conversion efficiency than PPy NPs and solid PLA@PPy NPs at each light power density. Since the mass of PPy NPs remained unchanged, the high conversion efficiency suggests that porous structure tailors more photons to be adsorbed by PPy NPs.

To identify the positive contribution of porous structure to the light trapping, light propagation through porous and solid PLA particles is compared. When an incident NIR light is illuminated on particles, it could be only reflected and scattered as PLA has no adsorption in the NIR region. The increased



DOI: 10.1021/acsmacrolett.5b00089
ACS Macro Lett. 2015, 4, 392−397

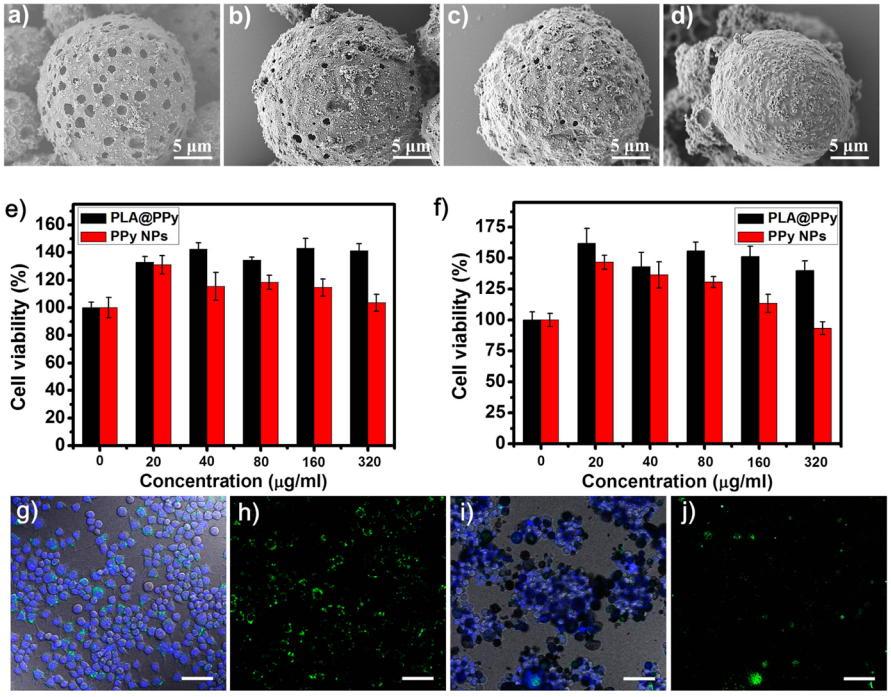


**Figure 4.** Self-closing process of porous PPy@PLA particles: (a) before NIR light illumination and after NIR light illumination (808 nm, 3.2 W/cm$^2$) for (b) 20 s, (c) 80 s, and (d) 120 s. Relative viabilities of macrophages that are incubated with PPy@PLA porous particles or PPy NPs for 12 h (e) and 24 h (f). Phagocytosis of Alexa 488-labeled DNA by macrophages: (g) An overlapped optical image of macrophages taking up DNA (green) in which the cell nucleus is dyed in blue; (h) A confocal florescent image to visualize DNA. (i) The overlapped optical image and (j) confocal fluorescent image of macrophages interacting with self-closed porous PPy@PLA particles loading DNA. Scale bar: 50 $\mu$m.

surface area facilitates the light reflection and scattering, prolonging the light pathway within the porous structure. Films composed of porous or nonporous PLA particles were exposed to a pulsed laser beam, and the reflected pulses were collected and analyzed in a time-resolved manner. As shown in Figure 3f, laser pulses reflected directly from the blank glass substrate exhibit pulse duration of 200 fs (blank trace, full width at half-maximum). However, those reflected from the films of nonporous or porous PLA particles show substantially extended trailing edges as indicated by the nonporous and porous traces. To be specific, the apparent decay time constants[28] are 1.66 and 0.46 ps for the porous and nonporous traces, respectively. Importantly, the area under curve (AUC) of the porous trace is 2.4 times larger than that of the nonporous one, and apparently, they are both much larger than the AUC of the blank substrate. The distinct AUC enhancement upon introducing porous structure is attributed to the occurrence of additional light migration. Such porous-structure-boosted light trapping provides more opportunities for polypyrrole to harvest photons, and thereby the conversion of light into heat energy becomes more efficient.

There exists a power density above which the change of conductivity stops increasing. As shown in Figure 3c, the conductivity change of PPy NPs and the PPy@PLA particle remains unchanged when the light power density is beyond 3.2 W/cm$^2$. It is hypothesized that thermal heat generated by polypyrrole reaches maximum, leading to a constant mobility of carriers. However, the conductivity change of porous PPy@PLA is declined when the power density is above this critical point. We attribute the decrease of conductivity change to the phase transition of porous PLA particles that is caused by photoannealing. As we reported previously,[13] excess heat as a result of photothermal conversion may close the surface pores if the local temperature is above the melting temperature ($T_m$) of PLA. To provide insight into this abnormal conductivity change, a thorough assessment is paid to the morphology of porous PPy@PLA under NIR illumination. As shown in Figure 4a–d, robust porous particles gradually closed their surface pores upon NIR irradiation. When a dose of NIR irradiation (3.2 W/cm$^2$, 2 min) is implemented, surface pores completely disappeared. At this state, local temperature reaches 270 °C as confirmed by an IR camera, which is much higher than the melting point of PLA. Hence we believe that the photothermal conversion of polypyrrole coating on the porous particles has generated enough heat to trigger the local motion of surface polymers.

Though the phase transition induced by photoannealing does not benefit the NIR sensing test at high light power density, the self-closing performance of porous PPy@PLA offers a remote way for controllable encapsulation of nucleic acids. An incentive of uncontrolled inflammation is considered due to redundant extracellular nucleic acids from a large area of dead and dying cells, which happens routinely to patients with severe burns or injuries.[29] It is generally believed that locally enriched nucleic acids may cause a disorder of the immune system if they are cleaned up by macrophages unusually. Self-closing porous particles are proposed as good candidates for reducing the risk of uncontrolled inflammation because they may capture and seal nucleic acids.

The cytotoxicity of the porous PPy@PLA particles by using macrophages is investigated before considering their full potential for biological applications. As shown in Figure 4e and 4f, the relative viabilities of the macrophages in the presence of porous PPy@PLA particles or PPy NPs with a range of concentrations were analyzed. Under incubation for 12 and 24 h or even extended times, both types of particles did not


DOI: 10.1021/acsmacrolett.5b00089
ACS Macro Lett. 2015, 4, 392−397

exhibit toxicity to macrophages from the assays. In contrast to PPy NPs, porous PPy@PLA particles cause little side effect to the cell proliferation as these polymer particles with an average size of 15 $\mu$m could not be taken up by cells. The inhibition of phagocytosis may avoid the serious immune response with the use of polymer particles. In addition to macrophages, human umbilical vein endothelial cells (HUVECs) are also treated with porous PPy@PLA particles to more clearly identify the nontoxicity of these hybrid polymer particles (Figure S11, Supporting Information).

The phagocytosis of nucleic acids from injured tissues is considered as the key step to decide the degree of inflammation. Therefore, self-closing polymer particles with a porosity of 85.5% (Figure S12, Supporting Information) render the possibility to inhibit the uncontrolled inflammation if they can effectively remove the nucleic acids. Macrophages generally act as the scavenger to take up the redundant nucleic acids in the vicinity of injuries before these nucleic acids travel into the bloodstream. To prevent the excessive phagocytosis, it is essential for self-closing particles to trap and lock the nucleic acids. We prepared a powder of porous PPy@PLA particles via lyophilization to examine their capability of trapping DNA. It is assumed that BSA acting as a surfactant has been encapsulated in the emulsion droplets and deposited on the external and internal surfaces within the porous structure. Noting that polymerization of pyrrole occurs at a low pH, BSA should be protonated below its isoelectric point, endowing the particle with a positively charged interior. This surface modification may provide a driving force to load DNA into PPy@PLA particles on the basis of electrostatic interaction. As shown in Figure 4g and 4h, the fluorescence-labeled DNA could be entirely loaded into macrophages after 1 h incubation. In contrast, porous PPy@PLA particles could load DNA more rapidly, and over 90% DNA molecules were loaded into the porous particles costing only a few seconds after the particle powder is dispersed (Figure S13, Supporting Information). Closing surface pores under NIR irradiation ensures the encapsulated DNA molecules to be permanently sealed in the polymer particles. No DNA was transferred into the cytoplasm of the macrophage after the closed particles were incubated with macrophages for 1 h (Figure 4i and 4j). Regarding that the polymer particles are large enough to escape phagocytosis, the nucleic acids will be ideally isolated from the immune system.

In conclusion, we have demonstrated a strategy for improving the NIR light sensitivity of the conducting polymer on porous polymer particles. We developed a method of one-step double emulsion with the use of natural protein as surfactants intending to prepare a class of conducting porous particles. The ease of preparation, combined with the high throughput of this emulsion method, offers a straightforward and generally applicable way for producing high-performance NIR-responsive materials. Controlled porous morphology affords the function of enhancing light reflection and diffraction, thus prolonging the light pathway within the polymer matrix. As a result of light trapping, the photothermal conversion efficiency of polypyrrole coating on the porous particles is remarkably improved, which fulfills the sensing and clinical applications of porous particles. It is found that the conductivity of polypyrrole increases under NIR irradiation owing to the photothermal conversion, offering great convenience to prepare cost-effective and flexible paper-based NIR light sensors. Excessive NIR irradiation is able to cause the phase transition of the polymer matrix. In comparison with thermal or solvent annealing, photoannealing is more possible to regulate phase transition in biological systems in consideration of less damage and strong penetration of NIR light. Self-closing of porous particle is achieved which is promising for capturing and sealing nucleic acids from injured tissues. It is envisioned that NIR-responsive porous particles could be readily extended for curing inflammatory diseases or regulating enzymatic reactions.

## ■ ASSOCIATED CONTENT

### Ⓢ Supporting Information

Experimental details and supporting figures. This material is available free of charge via the Internet at http://pubs.acs.org.

## ■ AUTHOR INFORMATION

### Corresponding Authors

*E-mail: yapeiwang@ruc.edu.cn.

*E-mail: zwsun@ccmu.edu.cn.

### Notes

The authors declare no competing financial interest.

## ■ ACKNOWLEDGMENTS

This work was financially supported by the National Natural Science Foundation of China (51373197, 21422407) and Trans-Century Training Programme Foundation for the Talents by the State Education Commission (NCET-12-0530).

## ■ REFERENCES

(1) Au, K.; Lu, Z.; Matcher, S. J.; Armes, S. P. *Adv. Mater.* **2011**, *23*, 5792−5795.

(2) Becker, A.; Hessenius, C.; Licha, K.; Ebert, B.; Sukowski, U.; Semmler, W.; Wiedenmann, B.; Grötzinger, C. *Nat. Biotechnol.* **2001**, *19*, 327−331.

(3) Vogel, A.; Venogopalan, V. *Chem. Rev.* **2003**, *103*, 577−64.

(4) Tao, P.; Shang, W.; Song, C.; Shen, Q.; Zhang, F.; Luo, Z.; Yi, N.; Zhang, D.; Deng, T. *Adv. Mater.* **2015**, *27*, 428−463.

(5) Kahl, T.; Bousack, H.; Schneider, E.; Schmitz, H. *Sensor Rev.* **2014**, *34*, 123−134.

(6) Weissleder, R. *Nat. Biotechnol.* **2001**, *19*, 316−317.

(7) Zhang, Z.; Wang, J.; Chen, C. *Adv. Mater.* **2013**, *25*, 3869−3880.

(8) Qian, G.; Wang, Z. Y. *Chem.—Asian J.* **2010**, *5*, 1006.

(9) Liu, Y.; Ai, K.; Lu, L. *Chem. Rev.* **2014**, *114*, 5057−5115.

(10) Pawlicki, M.; Collins, H. A.; Denning, R. G.; Anderson, H. L. *Angew. Chem., Int. Ed.* **2009**, *48*, 3244−3266.

(11) Liu, Q.; Feng, W.; Yang, T.; Yi, T.; Li, F. *Nat. Protoc.* **2013**, *8*, 2033−2044.

(12) Huang, X.; Qian, Q.; Zhang, X. Y.; Du, W.; Xu, H.; Wang, Y. *Part. Part. Syst. Charact.* **2013**, *30*, 235−240.

(13) Qian, Q.; Huang, X.; Zhang, X.; Xie, Z.; Wang, Y. *Angew. Chem., Int. Ed.* **2013**, *52*, 10625−10629.

(14) Tian, Q.; Tang, M.; Sun, Y.; Zou, R.; Chen, Z.; Zhu, M.; Yang, S.; Wang, J.; Wang, J.; Hu, J. *Adv. Mater.* **2011**, *23*, 3542−3547.

(15) Wu, M.-C.; Deokar, A. R.; Liao, J.-H.; Shih, P.-Y.; Ling, Y.-C. *ACS Nano* **2013**, *7*, 1281−1290.

(16) Dhar, N. K.; Dat, R.; Sood, A. K. *Optoelectronics- Advanced Materials and Devices*; InTech: Rijeka, Croatia, 2013.

(17) Jia, H.; Wang, J.; Zhang, X.; Wang, Y. *ACS Macro Lett.* **2014**, *3*, 86−90.

(18) Qian, Q.; Wang, J.; Yan, F.; Wang, Y. *Angew. Chem., Int. Ed.* **2014**, *53*, 4465−4468.

(19) Jia, H.; He, Y.; Zhang, X.; Du, W.; Wang, Y. *Adv. Electron. Mater.* **2015**, *1*, 1500029.

(20) Dawson, C.; Vincent, J. F.; Jeronimidis, G.; Rice, G.; Forshaw, P. *J. Theor. Biol.* **1999**, *199*, 291−295.

(21) Stegmaier, T.; Linke, M.; Planck, H. *Philos. Trans. R. Soc. A* **2009**, *367*, 1749−1758.



DOI: 10.1021/acsmacrolett.5b00089
*ACS Macro Lett.* 2015, 4, 392−397

(22) Zhang, X.; Ji, D.; Lei, T.; Zhao, B.; Song, K.; Hu, W.; Wang, J.-Y.; Pei, J.; Wang, Y. *J. Mater. Chem. A* **2013**, *1*, 10607−10611.
(23) Aizenberg, J.; Tkachenko, A.; Weiner, S.; Addadi, L.; Hendler, G. *Nature* **2001**, *412*, 819−822.
(24) Wang, Q.-L.; He, J.-H.; Li, Z.-B. *Therm. Sci.* **2012**, *16*, 339−342.
(25) Hiller, J.; Mendelsohn, J. D.; Rubner, M. F. *Nat. Mater.* **2002**, *1*, 59−63.
(26) Hu, L.; Chen, M.; Shan, W.; Zhan, T.; Liao, M.; Fang, X.; Hu, X.; Wu, L. *Adv. Mater.* **2012**, *24*, 5872−5877.
(27) Wang, J.; Zhang, X.; Huang, X.; Wang, S.; Qian, Q.; Du, W.; Wang, Y. *Small* **2013**, *9*, 3759−3764.
(28) Neves-Petersen, M. T.; Gryczynski, Z.; Lakowicz, J.; Fojan, P.; Pedersen, S.; Petersen, E.; Petersen, S. B. *Protein Sci.* **2009**, *11*, 588−600.
(29) Lee, J.; Sohn, J. W.; Zhang, Y.; Keong, K. W.; Pisetsky, D.; Sullenger, B. *Proc. Natl. Acad. Sci. U.S.A.* **2011**, *108*, 14055−14060.



DOI: 10.1021/acsmacrolett.5b00089
*ACS Macro Lett.* 2015, 4, 392−397